ACS OMEGA
Cite This: ACS Omega 2018, 3, 8583−8588
Article
http://pubs.acs.org/journal/acsodf

Lithium Metal Battery Using $LiFe_{0.5}Mn_{0.5}PO_4$ Olivine Cathode and Pyrrolidinium-Based Ionic Liquid Electrolyte

Daniele Di Lecce[†] and Jusef Hassoun*[,†,‡]

[†]Department of Chemical and Pharmaceutical Sciences and [‡]National Interuniversity Consortium of Materials Science and Technology (INSTM) University of Ferrara Research Unit, University of Ferrara, Via Fossato di Mortara, 17, 44121 Ferrara, Italy

ABSTRACT: Ionic liquids (ILs) represent the most suitable electrolyte media for a safe application in high-energy lithium metal batteries because of their remarkable thermal stability promoted by the room-temperature molten salt nature. In this work, we exploit this favorable characteristic by combining a pyrrolidinium-based electrolyte and a $LiFe_{0.5}Mn_{0.5}PO_4$ mixed olivine cathode in a lithium metal cell. The IL solution, namely *N*-butyl-*N*-methylpyrrolidinium bis(trifluoromethanesulfonyl)imide ($Pyr_{14}TFSI$) dissolving LiTFSI, is designed as viscous electrolyte, particularly suited for cells operating at temperatures higher than 40 °C, as demonstrated by electrochemical impedance spectroscopy. The olivine electrode, characterized by remarkable structural stability at high temperature, is studied in the lithium metal cell using the $Pyr_{14}TFSI$−LiTFSI medium above the room temperature. The Li/$Pyr_{14}TFSI$−LiTFSI/$LiFe_{0.5}Mn_{0.5}PO_4$ cell delivers a capacity of about 100 mA h g^{-1} through two voltage plateaus at about 3.5 and 4.1 V, ascribed to the iron and manganese redox reaction, respectively. The cycling stability, satisfactory levels of the energy density, and a relevant safety content suggest the cell studied herein as a viable energy storage system for future applications.

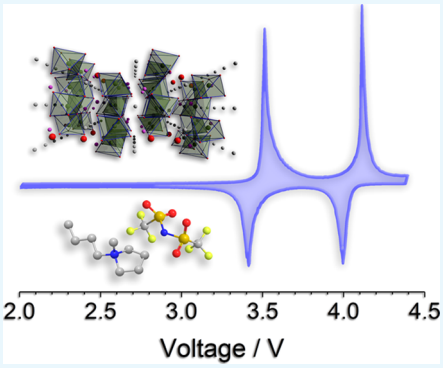

1. INTRODUCTION

Nowadays, the lithium-ion battery powers the most efficient and long-range electric vehicles, which actually reach an autonomy exceeding 300 km by a single charge.[1,2] Further increase of the driving range may be achieved by using the lithium battery, that is, the system in which the anode is represented by the light, highly energetic, while extremely reactive, lithium metal.[3,4] However, the use of this metal poses serious safety issues, including possible thermal runway due to short circuits promoted by dendrite formation or cell case damage.[5] Therefore, safe electrolytes, characterized by high boiling point as well as by low volatility, vapor pressure, and flammability, play a key role in determining the possible large scale diffusion of the rechargeable lithium metal battery.[6] Among the various alternatives proposed for achieving this challenging goal,[7−11] the room-temperature ionic liquids (ILs) represent very attracting solution because of their intrinsic thermal stability.[12,13] So far, the study of the IL-based electrolytes involved aprotic species formed by an organic cation and large anion, characterized by low Lewis basicity. The IL composition has a remarkable effect on several electrolyte properties, such as viscosity, conductivity, and electrochemical stability window, thus strongly affecting the cell performance. As for the cation, aliphatic quaternary ammonium, including pyrrolidinium and piperidinium, and aliphatic quaternary phosphonium have shown suitable low-voltage stability, while long alkyl chains typically lead to viscosity increase and conductivity decrease. On the other hand, amide and imide type anions generally ensure high anodic stability and satisfactory Li^+ transport.[14−17] Recently, *N*-butyl-*N*-methylpyrrolidinium bis(trifluoromethanesulfonyl)-imide ($Pyr_{14}TFSI$), *N*-butyl-*N*-methylpyrrolidinium bis-(fluorosulfonyl)imide ($Pyr_{14}FSI$), *N*-methoxy-ethyl-*N*-methyl-pyrrolidinium bis(trifluoromethanesulfonyl)imide ($Pyr_{12O1}TFSI$), and *N*-*N*-diethyl-*N*-methyl-*N*-(2-methoxyethyl)ammonium bis(trifluoromethanesulfonyl)imide ILs dissolving LiTFSI salt have demonstrated exceptional performance in lithium-ion batteries.[18,19] Among them, $Pyr_{14}TFSI$ revealed very promising characteristics in terms of chemical and electrochemical stability, however with a relatively high viscosity,[18] which may lead to low electrode wetting degree and high resistance during the electrochemical process, reflected into high cell polarization and low capacity. This issue may be actually mitigated by raising the operating temperature to a value higher than 40 °C, which is a condition easily reached in electric vehicles.[20] Olivine-framework cathodes with chemical formula $LiMPO_4$, where M represents a transition metal, are among the most suitable materials for ensuring long-life and safe lithium batteries because of the relevant stability of the phosphate (PO_4) group.[21] In particular, $LiFePO_4$ is the material of choice for commercial batteries, with a working voltage of about 3.5 V, a specific capacity of 170 mA h g^{-1}, and a theoretical energy of about 590 W h kg^{-1}.[2] These characteristics lead to a practical energy density of about 190 W h kg^{-1} and to remarkably long cycle life.[2] The energy density of the lithium cell may be further increased by

Received: June 13, 2018
Accepted: July 20, 2018
Published: August 1, 2018

DOI: 10.1021/acsomega.8b01328
ACS Omega 2018, 3, 8583−8588

partially replacing Fe in the olivine material with other transition metals having higher redox potential, such as Mn (E = 4.2 V vs Li^+/Li) and Co (E = 4.8 V vs Li^+/Li).[22,23]

In this work, we study a lithium metal battery that uses $Pyr_{14}TFSI$ dissolving LiTFSI as the electrolyte and a $LiFe_{0.5}Mn_{0.5}PO_4$ olivine-structure material as the cathode. The electrolyte is designed with LiTFSI concentration of 0.1 mol kg^{-1}, which is a value lower than the typically studied one (i.e., 0.2 mol kg^{-1}),[24] in order to keep a moderate viscosity. Prior to use, the ionic conductivity of the electrolyte is measured, while the lithium cell is studied at a temperature value of about 45 °C in order to favor electrode wetting, as verified by electrochemical impedance spectroscopy (EIS). The cell is galvanostatically cycled at C/5 and C/3 rate (1 C = 170 mA g^{-1}) and proposed as a safe energy storage system combining the modified olivine cathode, the IL-based electrolyte, and the high-energy lithium metal anode.

2. RESULTS AND DISCUSSION

The $Pyr_{14}TFSI$, LiTFSI 0.1 mol kg^{-1} electrolyte is studied in terms of conductivity to determine its applicability in a lithium battery through EIS on a symmetrical coin-cell using stainless steel electrodes (Figure 1). The Nyquist plots of the cell at

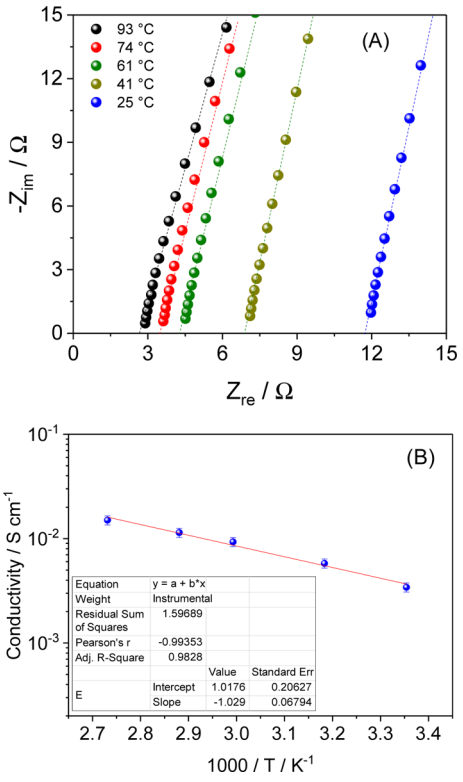

Figure 1. (A) Evolution of the EIS Nyquist plots over the temperature of the $Pyr_{14}TFSI$, LiTFSI 0.1 mol kg^{-1} electrolyte in a symmetrical stainless steel 2032 coin-cell and (B) corresponding Arrhenius conductivity plot. Frequency range: 100 kHz to 100 Hz. Signal amplitude: 10 mV.

various temperatures (Figure 1A) have the typical slope of a blocking-electrode cell approaching 90°, where the intercept indicates the electrolyte resistance. The corresponding conductivity, measured from room temperature to 90 °C, evidences an Arrhenius trend with high values ranging from about 3 × 10^{-3} S cm^{-1} at the room temperature to about 1 × 10^{-2} S cm^{-1} above 90 °C (Figure 1B). Nevertheless, more extended temperature range, particularly to the lower temperatures, indicated a Vogel−Tammann−Fulcher behavior rather than the Arrhenius one for this class of electrolytes.[18] On the other hand, the electrolyte conductivity is considered well suitable for application in lithium batteries, as indeed expected for the pyrrolidinium-based ILs.[14] It is worth mentioning that a high conductivity value and a decreased viscosity at moderately high temperature may allow an adequate electrode wetting for improving the cell performances.[19] Therefore, we have studied our lithium cell combining the $LiFe_{0.5}Mn_{0.5}PO_4$ cathode and the $Pyr_{14}TFSI$, LiTFSI electrolyte at a temperature of about 45 °C.

The $LiFe_{0.5}Mn_{0.5}PO_4$ electrode was prepared by the solvothermal technique reported in previous works.[21] Figure 2A, showing the transmission electron microscopy (TEM) image of the positive electrode powder, reveals uniform submicrometric platelets of $LiFe_{0.5}Mn_{0.5}PO_4$ surrounded by nanometric spherules of Super P carbon, which is used as the electron conducting additive (see Experimental Section for

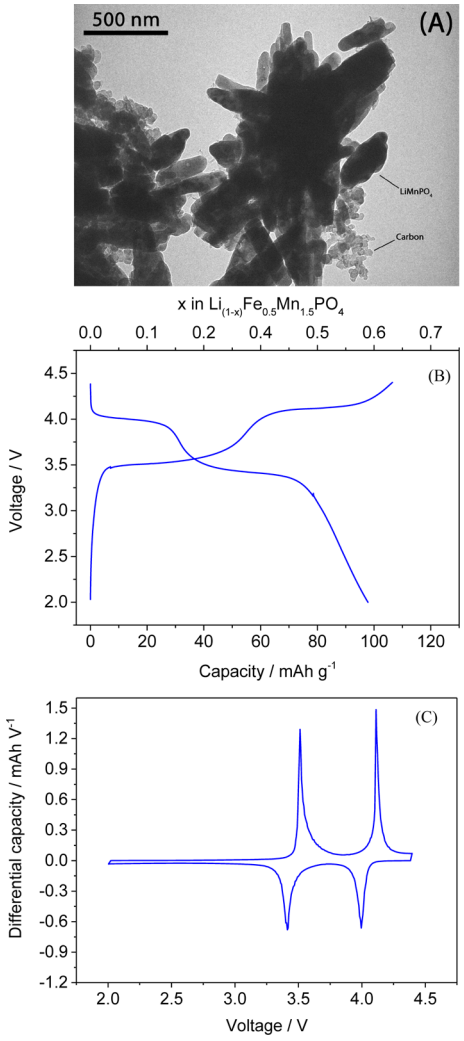

Figure 2. (A) TEM image of the $LiFe_{0.5}Mn_{0.5}PO_4$ electrode. Voltage profile (B) and differential capacity versus voltage (C) of a steady-state galvanostatic cycle of the Li/$Pyr_{14}TFSI$, LiTFSI 0.1 mol kg^{-1}/$LiFe_{0.5}Mn_{0.5}PO_4$ cell performed at a current of 21 mA g^{-1} (C/8 rate). Temperature: 45 °C. Voltage range: 2−4.4 V.

DOI: 10.1021/acsomega.8b01328
ACS Omega 2018, 3, 8583−8588

further details). This morphology is generally reflected into good electrochemical behavior of the material in the lithium cell,[21] as indeed suggested by Figure 2B,C, which report the voltage profile and the differential curve corresponding to a steady-state galvanostatic cycle of the Li/Pyr_{14}TFSI, LiTFSI 0.1 mol kg^{-1}/$LiFe_{0.5}Mn_{0.5}PO_4$ cell performed at a current of about 21 mA g^{-1} (C/8 rate) and a temperature of 45 °C. Figure 2B indicates a reversible exchange of 0.6 lithium equivalents by the $LiFe_{0.5}Mn_{0.5}PO_4$ material and a corresponding capacity of about 100 mA h g^{-1}. This value is lower than the theoretical one (170 mA h g^{-1}) and the value the material reaches in conventional carbonate-based electrolyte (corresponding to a lithium exchange higher than 0.7 equivalents),[21] as most likely due to a relatively low electrode-wetting ability of the selected IL. However, the low electrode wetting by the viscose IL-based electrolyte might not be the only parameter determining the cell performance. Another important characteristic which may reasonably limit the charge transfer at the electrode/electrolyte interphase, thus the cell capacity, is the relatively low transport number of Li^+ ions expected for the IL-based solutions compared to the alkyl carbonate- and glyme-based electrolytes because of the molten salt nature of the ILs in which several ions contribute to the charge transport.[27] On the other hand, the low flammability and the high thermal stability of the Pyr_{14}TFSI−LiTFSI solution with respect to the conventional electrolytes based on organic carbonate solvents, such as ethylene carbonate and dimethyl carbonate,[28] well justify its use in a cell employing a highly reactive lithium metal anode. Furthermore, the differential curve of Figure 2C reveals a reversible operation of the cell at about 3.5 and 4.1 V, that is, a higher working voltage compared to the $LiFePO_4$ material owing to the redox activity of the Fe^{3+}/Fe^{2+} and Mn^{3+}/Mn^{2+} couples.[22]

The key role of the electrode/electrolyte interphase in determining the cell behavior has been verified by EIS of the Li/Pyr_{14}TFSI, LiTFSI 0.1 mol kg^{-1}/$LiFe_{0.5}Mn_{0.5}PO_4$ cell at temperature increasing from 23 °C (Figure 3A), to 40 °C (Figure 3B), 50 °C (Figure 3C), and 60 °C (Figure 3D). The spectra have been analyzed by the nonlinear least squares (NLLS) method using the equivalent circuit shown in Figure 3E. Among the various models proposed for impedance interpretation,[29] we have adopted in this work an equivalent circuit taking into account the high-frequency electrolyte resistance, the high-middle frequency contribution of constant phase elements (CPE_1 and CPE_2) and resistances (R_{i1} and R_{i2}) ascribed to the electrode/electrolyte interphases, and a low-frequency pseudo-capacitance attributed either to the Li^+ diffusion or the Li^+ accumulation into the electrode.[30] Accordingly, the overall electrode/electrolyte interphase resistance (R_i) has been calculated considering both R_{i1} and R_{i2}, and reported in Figure 3E as a function of temperature. EIS reveals a significant decrease of R_i from 580 ± 60 Ω at the room temperature to 166 ± 3 Ω at 93 °C according to an asymptotic trend, as shown in Figure 3E. We reasonably assume that the impedance drop may be ascribed to an increase of the electrode wetting by the IL at high temperature.[18] However, beneficial effects of the raising temperature on both the ionic and the electronic conductivities of the $LiFe_{0.5}Mn_{0.5}PO_4$ electrode can be also expected.[31] It is noteworthy that the electrolyte viscosity has a direct effect on both the ionic conductivity and the wetting ability of electrode and separator, thus significantly affecting the rate capability of lithium cells. In particular, low viscosity and high wetting

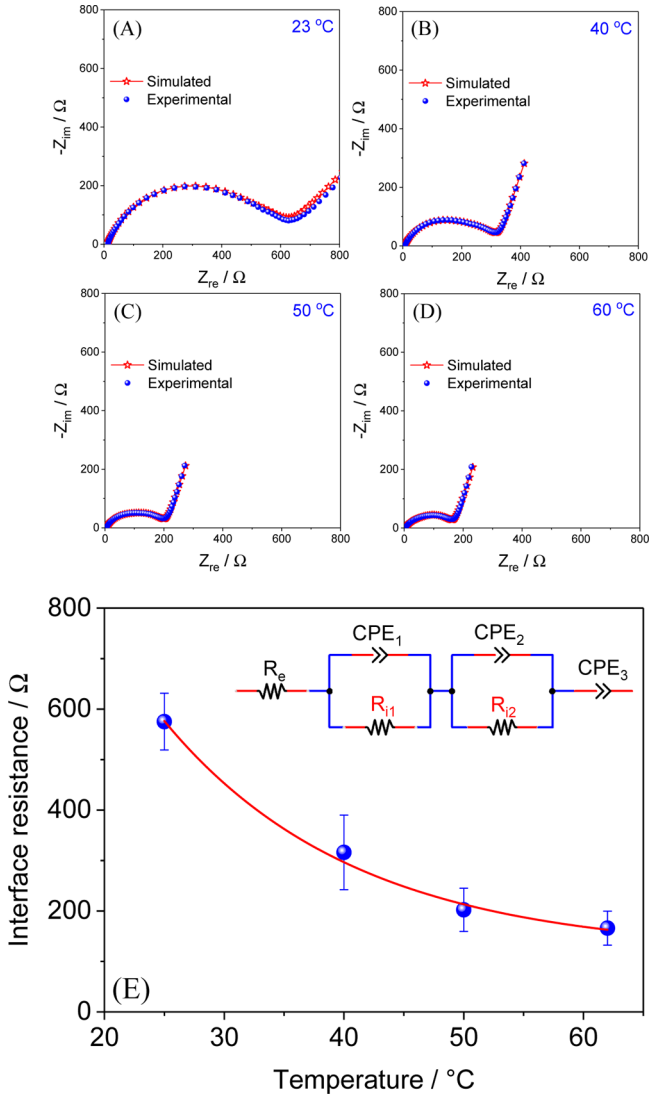

Figure 3. Experimental and simulated Nyquist plots related to electrochemical impedance spectra of the Li/Pyr_{14}TFSI, LiTFSI 0.1 mol kg^{-1}/$LiFe_{0.5}Mn_{0.5}PO_4$ cell at (A) 23, (B) 40, (C) 50, and (D) 60 °C; the spectra have been analyzed by the NLLS method using the Boukamp package.[25,26] (E) Trend of the interface resistance reported as a function of temperature, and equivalent circuit employed for the NLLS analysis in inset. Frequency range: 500 kHz to 100 mHz. Signal amplitude: 10 mV.

ability improve the rate capability and decrease the cell polarization.[18] We point out that temperatures of the order of 40 °C are usually reached in electric vehicles during driving stages or achieved by using relatively simple heating tools in cold climate conditions. Furthermore, active cooling systems are actually required to mitigate the battery decay due to possible decomposition of electrolyte at operating temperature peaks, which may lead to irregular solid electrolyte interphase (SEI) layer growth upon cycling.[20] Therefore, the temperature employed in this work, that is, 45 °C, is considered a suitable value, appropriate for efficient use of the IL-based energy storage systems.

Galvanostatic cycling test of the Li/Pyr_{14}TFSI, LiTFSI 0.1 mol kg^{-1}/$LiFe_{0.5}Mn_{0.5}PO_4$ cell is performed at 45 °C using current rates of C/3 and C/5 (1 C = 170 mA g^{-1}). The voltage profile of the cell reported in Figure 4A reveals the above-

DOI: 10.1021/acsomega.8b01328
ACS Omega 2018, 3, 8583−8588

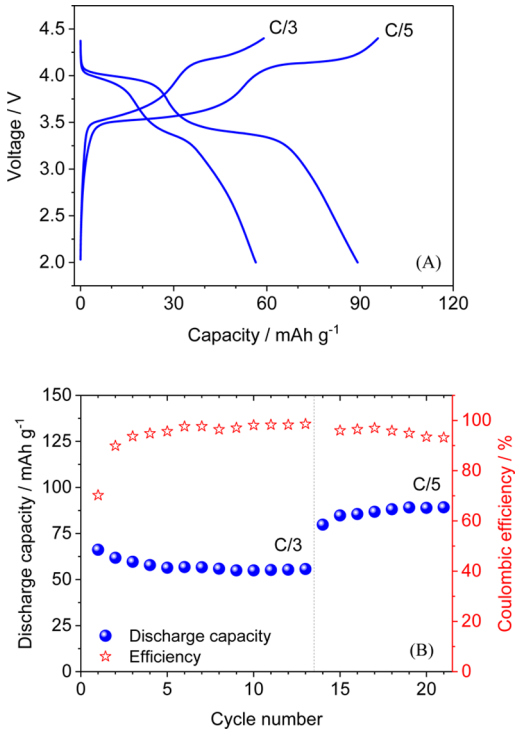

Figure 4. (A) Voltage profile and (B) cycling trend with Coulombic efficiency of the galvanostatic test of the Li/Pyr_{14}TFSI, LiTFSI 0.1 mol kg^{-1}/$LiFe_{0.5}Mn_{0.5}PO_4$ cell performed at C/3 and C/5 rates (1 C = 170 mA g^{-1}). Temperature: 45 °C. Voltage range: 2−4.4 V.

mentioned two voltage plateaus evolving at about 3.5 and 4.1 V, a moderate polarization between charge and discharge, and a reversible specific capacity of about 60 and 90 mA h g^{-1} at C/3 and C/5 rates. Hence, the cell using the $LiFe_{0.5}Mn_{0.5}PO_4$ electrode and the IL electrolyte reaches the 35 and 53% of the theoretical capacity at C/3 and C/5 rates, respectively.[21] Figure 4B indicates a stable cycling trend at C/3 rate after the first cycle, which is characterized by a discharge capacity of 66 mA h g^{-1} and a low Coulombic efficiency (70%) because of partial electrolyte oxidation to form a stable SEI layer.[18] Subsequently, the cell shows slightly lower capacity and higher Coulombic efficiency of 98%. The capacity increases to 90 mA h g^{-1} and the Coulombic efficiency slightly decreases (95%) as the C-rate is lowered to C/5 at the 14th cycle. Hence, the galvanostatic test of Figure 4 suggests the applicability of the adopted electrode/electrolyte combination as an energy storage system by further improving the delivered capacity. As already mentioned, the wetting ability of the electrolyte solution plays a crucial role in determining the electrode/electrolyte interphase resistance and affects the cell performance in terms of delivered capacity. Accordingly, the $LiMn_{0.5}Fe_{0.5}PO_4$ electrode has shown higher capacity in different cell configurations previously reported, using alkyl carbonate- and glyme-based electrolytes that have lower viscosity than the Pyr_{14}TFSI−LiTFSI solution.[21,32,33] Thus, proper tuning the IL electrolyte viscosity and wetting-ability, for example, by changing either its chemical composition or the lithium salt concentration, is expected to improve the cell performance.[18] Besides electrolyte optimization, fine material engineering might effectively mitigate the low electronic conductivity and Li^+ transport limits of $LiMn_{1-x}Fe_xPO_4$ phases, thereby further enhancing rate capability and specific capacity of the cell.[34,35]

3. CONCLUSIONS

We proposed herein a lithium battery combining a pyrrolidinium-based IL electrolyte and a modified olivine cathode including iron and manganese, that is, Pyr_{14}TFSI−LiTFSI and $LiFe_{0.5}Mn_{0.5}PO_4$, respectively. The electrolyte showed a conductivity ranging from 10^{-3} S cm^{-1} at room temperature to 10^{-2} S cm^{-1} at about 90 °C. The cell delivered a maximum capacity approaching 100 mA h g^{-1} through two voltage plateaus at about 3.5 and 4.1 V, hence with theoretical energy density of about 400 W h kg^{-1} and a practical energy exceeding 120 W h kg^{-1}. The results evidenced the decrease of cell impedance by raising temperature, thus suggesting the viscosity and the wetting-ability of the IL at the electrode/electrolyte interphase as a key factor for further improving the cell performances. Therefore, the lithium metal cell studied in this work is considered as a new energy storage system which may be actually improved by properly modifying the IL to enhance the electrode/electrolyte interphase, thus increasing cell capacity and energy density. Several IL-based electrolytes and new cathode materials have been proposed so far.[18,21] Our results suggest that alternative combinations of these materials can actually promote the development of new, high-energy, and safe batteries using the light and efficient lithium metal anode.

4. EXPERIMENTAL SECTION

1-Butyl-1-methylpyrrolidinium bis(trifluoromethanesulfonyl)-imide (Pyr_{14}TFSI, Solvionic) and lithium bis-(trifluoromethanesulfonyl)imide (LiTFSI, Solvionic) were dried several days under vacuum at 60 and 110 °C, respectively. The electrolyte solution was prepared by dissolving 0.1 mol of LiTFSI in 1 kg of Pyr_{14}TFSI and further dried under vacuum overnight at 60 °C. The $LiMn_{0.5}Fe_{0.5}PO_4$ powder was synthesized by the solvothermal pathway.[21] Lithium hydroxide monohydrate ($LiOH·H_2O$, Sigma-Aldrich), lithium dihydrogen phosphate (LiH_2PO_4, Sigma-Aldrich), manganese sulfate monohydrate ($MnSO_4·H_2O$, Sigma-Aldrich), iron sulfate heptahydrate ($FeSO_4·7H_2O$, Sigma-Aldrich), and sucrose were added to a 2:1 v/v ethylene glycol/H_2O solution under stirring in order to get a suspension. The molar ratios of LiH_2PO_4, $MnSO_4·H_2O$, $FeSO_4·7H_2O$, $LiOH·H_2O$, and sucrose were 1:0.5:0.5:1.75:0.03. The suspension was sealed into a Teflon-lined autoclave and heated in an oven at 180 °C for 20 h to get a $LiMn_{0.5}Fe_{0.5}PO_4$ precursor,[21] which was filtered, washed with water and ethanol, and dried in the oven overnight at 70 °C. The $LiMn_{0.5}Fe_{0.5}PO_4$ precursor was carbon-coated (about 5 wt % of C)[21] by precipitating sucrose over the olivine powder in a sucrose/water solution (molar ratio $LiMn_{0.5}Fe_{0.5}PO_4$/sucrose = 80:20% w/w), and then by heating the resulting composite at 700 °C for 3 h under an Ar atmosphere.

The positive electrode was prepared by doctor-blade coating on an aluminum current collector foil. The electrode slurry was prepared by mixing $LiMn_{0.5}Fe_{0.5}PO_4$, poly(vinylidene difluoride)-hexafluoropropylene (Kynar Flex 2801), and Super P carbon (Timcal) in the weight ratio 8:1:1 in tetrahydrofuran (Sigma-Aldrich). The coated electrode foil was cut into the form of disks, which were dried for 3 h under vacuum at 110 °C. The active material loading of the electrodes was about 2.3 mg cm^{-2}. The positive electrode morphology was investigated by TEM by entrapping the sample into a Formvar support. TEM images were taken through a Zeiss EM 910 microscope

DOI: 10.1021/acsomega.8b01328
ACS Omega 2018, 3, 8583−8588

equipped with a tungsten thermionic electron gun operating at 100 kV.

CR2035 coin-cells (MTI) were assembled in an Ar-filled glovebox (MBraun, O_2 and H_2O content below 1 ppm) by using a lithium metal disk as the anode, a Whatman GF/D glass fiber separator soaked by the $Pyr_{14}TFSI$, LiTFSI 0.1 mol kg^{-1} electrolyte, and the $LiMn_{0.5}Fe_{0.5}PO_4$ electrode as the cathode. The ionic conductivity of the $Pyr_{14}TFSI$, LiTFSI 0.1 mol kg^{-1} electrolyte was measured by EIS within the temperature range from 25 to 93 °C, by applying an alternate signal of 10 mV amplitude from 100 kHz to 100 Hz. The EIS measurements have been carried out on a symmetrical stainless steel blocking CR2032 coin-cell, employing a Teflon ring spacer to fix the cell constant (4.0×10^{-2} cm^{-1}). Further EIS measurements were carried out on the Li/$Pyr_{14}TFSI$, LiTFSI 0.1 mol kg^{-1}/$LiFe_{0.5}Mn_{0.5}PO_4$ cell at 23, 40, 50, and 60 °C, by applying an alternate signal of 10 mV amplitude from 500 kHz to 100 mHz. The impedance spectra were recorded through a VersaSTAT MC Princeton Applied Research (PAR) potentiostat and analyzed by the NLLS method using the Boukamp package.[25,26] The Li/$Pyr_{14}TFSI$, LiTFSI 0.1 mol kg^{-1}/$LiFe_{0.5}Mn_{0.5}PO_4$ cell was tested by galvanostatic cycling at 45 °C within the voltage range from 2 to 4.4 V, using the C/8, C/5, and C/3 rates (1 C = 170 mA g^{-1}). The galvanostatic cycling experiments have been performed through a MACCOR Series 4000 battery test system.

AUTHOR INFORMATION

Corresponding Author

*E-mail: jusef.hassoun@unife.it (J.H.).

ORCID

Daniele Di Lecce: 0000-0003-1290-1140

Jusef Hassoun: 0000-0002-8218-5680

Notes

The authors declare no competing financial interest.

ACKNOWLEDGMENTS

The work was carried out within the collaboration project "Accordo di Collaborazione Quadro 2015" between the University of Ferrara (Department of Chemical and Pharmaceutical Sciences) and the Sapienza University of Rome (Department of Chemistry) and supported by the grant "Fondo di Ateneo per la Ricerca Locale (FAR) 2017".

REFERENCES

(1) Andre, D.; Kim, S.-J.; Lamp, P.; Lux, S. F.; Maglia, F.; Paschos, O.; Stiaszny, B. Future Generations of Cathode Materials: An Automotive Industry Perspective. *J. Mater. Chem. A* **2015**, *3*, 6709−6732.

(2) Di Lecce, D.; Verrelli, R.; Hassoun, J. Lithium-Ion Batteries for Sustainable Energy Storage: Recent Advances towards New Cell Configurations. *Green Chem.* **2017**, *19*, 3442−3467.

(3) Lin, D.; Liu, Y.; Cui, Y. Reviving the Lithium Metal Anode for High-Energy Batteries. *Nat. Nanotechnol.* **2017**, *12*, 194−206.

(4) Park, S.-J.; Hwang, J.-Y.; Yoon, C. S.; Jung, H.-G.; Sun, Y.-K. Stabilization of Lithium-Metal Batteries Based on the in Situ Formation of a Stable Solid Electrolyte Interphase Layer. *ACS Appl. Mater. Interfaces* **2018**, *10*, 17985−17993.

(5) Zhang, K.; Lee, G.-H.; Park, M.; Li, W.; Kang, Y. M. Recent Developments of the Lithium Metal Anode for Rechargeable Non-Aqueous Batteries. *Adv. Energy Mater.* **2016**, *6*, 1600811.

(6) Di Lecce, D.; Sharova, V.; Jeong, S.; Moretti, A.; Passerini, S. A Multiple Electrolyte Concept for Lithium-Metal Batteries. *Solid State Ionics* **2018**, *316*, 66−74.

(7) Di Girolamo, D.; Panero, S.; Navarra, M. A.; Hassoun, J. Quaternary Polyethylene Oxide Electrolytes Containing Ionic Liquid for Lithium Polymer Battery. *J. Electrochem. Soc.* **2016**, *163*, A1175−A1180.

(8) Kimura, K.; Yajima, M.; Tominaga, Y. A highly-concentrated poly(ethylene carbonate)-based electrolyte for all-solid-state Li battery working at room temperature. *Electrochem. Commun.* **2016**, *66*, 46−48.

(9) Hassoun, J.; Fernicola, A.; Navarra, M. A.; Panero, S.; Scrosati, B. An advanced lithium-ion battery based on a nanostructured Sn-C anode and an electrochemically stable LiTFSi-Py24TFSI ionic liquid electrolyte. *J. Power Sources* **2010**, *195*, 574−579.

(10) Tominaga, Y.; Yamazaki, K.; Nanthana, V. Effect of Anions on Lithium Ion Conduction in Poly(Ethylene Carbonate)-Based Polymer Electrolytes. *J. Electrochem. Soc.* **2015**, *162*, A3133−A3136.

(11) Yuuki, T.; Konosu, Y.; Ashizawa, M.; Iwahashi, T.; Ouchi, Y.; Tominaga, Y.; Ooyabu, R.; Matsumoto, H.; Matsumoto, H. Ionic Liquid-Based Electrolytes Containing Surface-Functionalized Inorganic Nanofibers for Quasisolid Lithium Batteries. *ACS Omega* **2017**, *2*, 835−841.

(12) Moreno, J. S.; Deguchi, Y.; Panero, S.; Scrosati, B.; Ohno, H.; Simonetti, E.; Appetecchi, G. B. N-Alkyl-N-ethylpyrrolidinium cation-based ionic liquid electrolytes for safer lithium battery systems. *Electrochim. Acta* **2016**, *191*, 624−630.

(13) Fernicola, A.; Croce, F.; Scrosati, B.; Watanabe, T.; Ohno, H. LiTFSI-BEPyTFSI as an Improved Ionic Liquid Electrolyte for Rechargeable Lithium Batteries. *J. Power Sources* **2007**, *174*, 342−348.

(14) Watanabe, M.; Thomas, M. L.; Zhang, S.; Ueno, K.; Yasuda, T.; Dokko, K. Application of Ionic Liquids to Energy Storage and Conversion Materials and Devices. *Chem. Rev.* **2017**, *117*, 7190−7239.

(15) Tokuda, H.; Hayamizu, K.; Ishii, K.; Susan, M. A. B. H.; Watanabe, M. Physicochemical Properties and Structures of Room Temperature Ionic Liquids. 2. Variation of Alkyl Chain Length in Imidazolium Cation. *J. Phys. Chem. B* **2005**, *109*, 6103−6110.

(16) Armand, M.; Endres, F.; MacFarlane, D. R.; Ohno, H.; Scrosati, B. Ionic-Liquid Materials for the Electrochemical Challenges of the Future. *Nat. Mater.* **2009**, *8*, 621−629.

(17) Galiński, M.; Lewandowski, A.; Stępniak, I. Ionic Liquids as Electrolytes. *Electrochim. Acta* **2006**, *51*, 5567−5580.

(18) Elia, G. A.; Ulissi, U.; Jeong, S.; Passerini, S.; Hassoun, J. Exceptional Long-Life Performance of Lithium-Ion Batteries Using Ionic Liquid-Based Electrolytes. *Energy Environ. Sci.* **2016**, *9*, 3210−3220.

(19) Elia, G. A.; Ulissi, U.; Mueller, F.; Reiter, J.; Tsiouvaras, N.; Sun, Y.-K.; Scrosati, B.; Passerini, S.; Hassoun, J. A Long-Life Lithium Ion Battery with Enhanced Electrode/Electrolyte Interface by Using an Ionic Liquid Solution. *Chem.—Eur. J.* **2016**, *22*, 6808−6814.

(20) Neubauer, J.; Wood, E. Thru-life impacts of driver aggression, climate, cabin thermal management, and battery thermal management on battery electric vehicle utility. *J. Power Sources* **2014**, *259*, 262−275.

(21) Di Lecce, D.; Fasciani, C.; Scrosati, B.; Hassoun, J. A Gel-Polymer Sn-C/LiMn0.5Fe0.5PO4 Battery Using a Fluorine-Free Salt. *ACS Appl. Mater. Interfaces* **2015**, *7*, 21198−21207.

(22) Oh, S.-M.; Jung, H.-G.; Yoon, C. S.; Myung, S.-T.; Chen, Z.; Amine, K.; Sun, Y.-K. Enhanced electrochemical performance of carbon-LiMn1−xFexPO4 nanocomposite cathode for lithium-ion batteries. *J. Power Sources* **2011**, *196*, 6924−6928.

(23) Di Lecce, D.; Brescia, R.; Scarpellini, A.; Prato, M.; Hassoun, J. A High Voltage Olivine Cathode for Application in Lithium-Ion Batteries. *ChemSusChem* **2016**, *9*, 223−230.

(24) Agostini, M.; Ulissi, U.; Di Lecce, D.; Ahiara, Y.; Ito, S.; Hassoun, J. A Lithium-Ion Battery based on an Ionic Liquid Electrolyte, Tin-Carbon Nanostructured Anode, and Li2O-ZrO2-Coated Li[Ni0.8Co0.15Al0.05]O2Cathode. *Energy Technol.* **2015**, *3*, 632−637.

DOI: 10.1021/acsomega.8b01328
ACS Omega 2018, 3, 8583−8588

(25) Boukamp, B. A Nonlinear Least Squares Fit Procedure for Analysis of Immittance Data of Electrochemical Systems. *Solid State Ionics* **1986**, *20*, 31−44.
(26) Boukamp, B. A Package for Impedance/Admittance Data Analysis. *Solid State Ionics* **1986**, *18−19*, 136−140.
(27) Kühnel, R.-S.; Balducci, A. Lithium Ion Transport and Solvation in N-Butyl-N-methylpyrrolidinium Bis-(trifluoromethanesulfonyl)imide-Propylene Carbonate Mixtures. *J. Phys. Chem. C* **2014**, *118*, 5742−5748.
(28) Arbizzani, C.; Gabrielli, G.; Mastragostino, M. Thermal Stability and Flammability of Electrolytes for Lithium-Ion Batteries. *J. Power Sources* **2011**, *196*, 4801−4805.
(29) Nara, H.; Morita, K.; Mukoyama, D.; Yokoshima, T.; Momma, T.; Osaka, T. Impedance Analysis of LiNi 1/3 Mn 1/3 Co 1/3 O 2 Cathodes with Different Secondary-particle Size Distribution in Lithium-ion Battery. *Electrochim. Acta* **2017**, *241*, 323−330.
(30) Aurbach, D. Review of selected electrode-solution interactions which determine the performance of Li and Li ion batteries. *J. Power Sources* **2000**, *89*, 206−218.
(31) Molenda, J.; Ojczyk, W.; Marzec, J. Electrical conductivity and reaction with lithium of LiFe1−yMnyPO4 olivine-type cathode materials. *J. Power Sources* **2007**, *174*, 689−694.
(32) Di Lecce, D.; Carbone, L.; Gancitano, V.; Hassoun, J. Rechargeable lithium battery using non-flammable electrolyte based on tetraethylene glycol dimethyl ether and olivine cathodes. *J. Power Sources* **2016**, *334*, 146−153.
(33) Carbone, L.; Di Lecce, D.; Gobet, M.; Munoz, S.; Devany, M.; Greenbaum, S.; Hassoun, J. Relevant Features of a Triethylene Glycol Dimethyl Ether-Based Electrolyte for Application in Lithium Battery. *ACS Appl. Mater. Interfaces* **2017**, *9*, 17085−17095.
(34) Oh, S.-M.; Myung, S.-T.; Park, J. B.; Scrosati, B.; Amine, K.; Sun, Y.-K. Double-Structured LiMn0.85Fe0.15PO4 Coordinated with LiFePO4 for Rechargeable Lithium Batteries. *Angew. Chem.* **2012**, *124*, 1889−1892.
(35) Di Lecce, D.; Hassoun, J. Lithium Transport Properties in LiMn1−αFeαPO4 Olivine Cathodes. *J. Phys. Chem. C* **2015**, *119*, 20855−20863.

DOI: 10.1021/acsomega.8b01328
ACS Omega 2018, 3, 8583−8588